PRODUCTION OF CHARM AND NEW PARTICLES IN NEUTRINO-NUCLEON INTERACTIONS

H. Eugene Fisk
Fermi National Accelerator Laboratory
P.O. Box 500
Batavia, IL 60510

Summary

The current experimental status of charm production by neutrinos is reviewed. Recent results on like-sign dimuons are also discussed.

I. Introduction

Since the 1979 Lepton Photon Conference several groups have presented new data on charm production by neutrinos[1]. This report will concentrate on three topics: (1) Explicit observations of charm production in the emulsion experiment at Fermilab (E531); (2) New data on opposite-sign dileptons with a discussion of the energy dependence of the charm production cross section, x distributions, charmed quark fragmentation, and the relative strength of the strange quark sea; and (3) Like-sign dileptons, their existence, background, and possible sources.

Charm as a fourth quark was suggested as early as 1964 and predictions of bare charmed-particle production by neutrinos were proposed in 1970 when Glashow, Illiopoulos, and Maiani (GIM) introduced the fourth quark and their mechanism for suppressing strangeness-changing neutral currents[2]. Theoretical predictions regarding the deep inelastic neutrino production of charm were made in 1974 by Altarelli et al., and Gaillard[3]. The standard model for weak interactions (Weinberg-Salam, GIM, Kobayashi-Maskawa[4]) provides a theoretical framework for charm production which involves the transition from a light quark, d or s, to the charmed quark, c, followed by fragmentation to a charmed hadron (see Figure 1). The charmed hadron subsequently decays weakly with the Cabibbo-allowed strange decay or Cabibbo-suppressed non-strange decay with a lifetime $\sim 10^{-13}$ seconds.

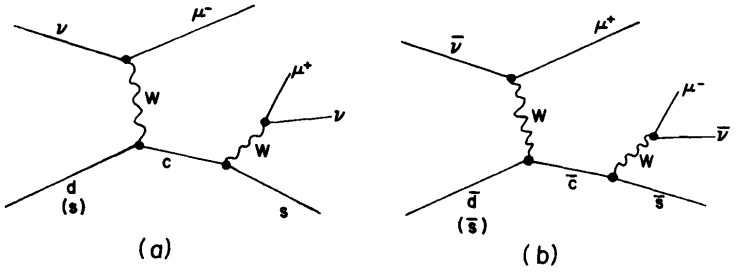

Fig. 1. Feynman diagrams for charm production by neutrinos(a) and antineutrinos(b). The neutrino rate is $\sim d(x)\sin^2\theta_c + s(x)\cos^2\theta_c$ while the antineutrino rate is $\sim \bar{d}(x)\sin^2\theta_c + \bar{s}(x)\cos^2\theta_c$.

II. Explicit Production of Charm

A. Old Data

The first explicit example of the production of charm by neutrinos was the BNL bubble chamber event[5] where $\nu p \to \mu^- \Sigma_c^{++}$ (2.426) which decayed to $\Lambda_c^+ \pi^+$ with the Λ_c^+ going to a Λ and three charged pions. This discovery was quickly followed by the first emulsion observation of what was surely charm production, although the charged 182μm track terminated in a decay which could not be uniquely identified[6]. In subsequent Columbia-BNL and BNL experiments evidence was presented for explicit production of: D^o (64 events above a background of 180 events)[7], Λ_c (2 unique events)[8], and Σ_c^{++} (20 events with a background of 6 events)[9]. At the time of the '79 Lepton-Photon Conference, the Fermilab emulsion experiment (E531) had observed 10 events ($1F^-$, $3D^+$, $1\Lambda_c$, and 4 D^o)[10] while the BEBC emulsion experiment reported 5 events (3 D^o, 1 Λ_c, 1 ambiguous)[11].

B. New Data on Explicit Production of Charm

The BEBC neutrino collaboration, ABCMO, has found 2 examples each of Λ_c^+, charmed baryon and D^{*+} charmed meson production[12]. Paper 9 contributed to this conference[13] reports the observation of a neutrino-produced Λ_c^+, which decays to $\Sigma^o \pi^+$. The emulsion experiment performed at Fermilab, E531, has now accumulated 44 events with explicit charm[14].

C. E531 Experiment

The experimental apparatus for E531 includes 31 liters of emulsion target, an open magnet instrumented upstream and downstream with drift chambers, time of flight counters for charged particle identification, lead glass for e and γ identification ($\Delta E = \pm 0.14\sqrt{E}$), a hadron calorimeter for neutral hadron identification ($\Delta E = \pm 1.1\sqrt{E}$), and a muon identifier with hodoscopes. The drift chambers and a changeable emulsion sheet with very few background tracks, allow the prediction of the interaction vertex to 0.5mm in the direction perpendicular to the neutrino beam. Once the interaction vertex is located, the charmed meson and baryon decays are found by searching the emulsion with two techniques. In the first method the charged tracks with polar angle less than 20^o are followed for 6mm, and neutral decay vertices are searched in a cyclindrical volume whose axis is along the ν beam direction, having a radius of 300μm and a length 1mm downstream of the production vertex. In the second search method they follow back each track, using the drift chambers and changeable fiducial sheet information, into the emulsion to its decay or production vertex. The efficiency vs. distance for finding decays is shown in Figure 2. For charged decays with three or more tracks leaving the vertex and neutral decays the efficiency is quite good downstream of the vertex clutter.

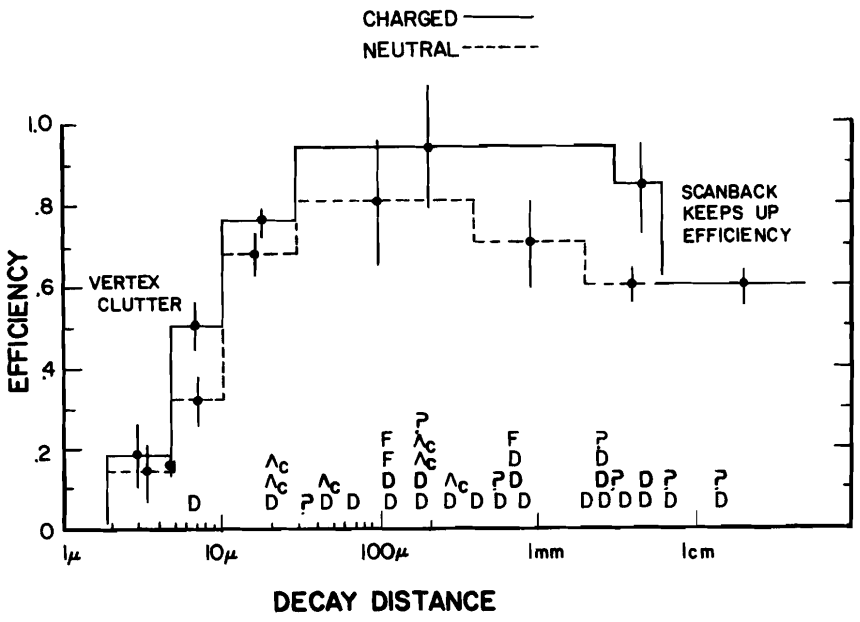

Fig. 2. E531 emulsion experiment efficiency for detecting decays of charmed hadrons. The ordinate is the logarithm of the decay length.

Table 1 summarizes the unambiguous events and their observed decay modes. Lifetimes are not given since they are discussed in these proceedings by L. Foa. There are three additional charged decay events which are ambiguous among D^+, F^+, and Λ_c^+ and seven events still being analyzed. The three $\bar{D}^o$ and the single D^- events are each accompanied by an identified μ^+ which implies they are initiated by $\bar{\nu}$. Flux calculations for the wide band beam indicate the $\bar{\nu}/\nu$ flux ratio is 0.07 with the $\bar{\nu}$ flux peaked toward higher energies. Thus the production ratio $\bar{D}/D$ is as expected. From the measured inclusive 3-prong branching ratio for the decay of charged D's (0.47) a total of ~8 D^+ is implied[16,17]. Six of the 17 D^o and $\bar{D}^o$ events result from the decay of a D^{*+}. If equal production of D^{*+} and D^{*o} is assumed, then from the known branching ratios of $D^{*o}\rightarrow D^o(100\%)$ and $D^{*+}\rightarrow D^o(64\%)$ the D^*/D production ratio is roughly 2.5 and the observed D^o/D^+ ratio is ~2.

Figure 3 shows the energy distribution of the single muon charged current (1μ) interactions and the charm production events. The 1μ events are required to have $p_\mu > 4$ GeV/c since the efficiency for observing a μ is significantly reduced below this cut. It should be noted that the Λ_c (cud

Table 1: E531 Emulsion Experiment Event Decay Modes

Λ_c ***	F
$\Lambda_c^+ \rightarrow$ p K^o	$F^- \rightarrow \pi^+\pi^-\pi^-\pi^o$
p $K^-\pi^+\pi^o$	$F^+ \rightarrow K^+\pi^+\pi^-\bar{K}^o$
2 p $\pi^+\pi^-\bar{K}^0$	$\rightarrow K^+K^-\pi^+\pi^o$
3 Λ $\pi^+\pi^-\pi^+$	$\rightarrow \pi^+\pi^+\pi^-\pi^o$ +
$\Sigma^o\pi^+$	
D^o or $\bar{D}^o$	D^+ or D^-
$D^o \rightarrow K^-\pi^+\pi^o$	$D^+ \rightarrow K^-\pi^+\pi^+\pi^o$
$K^-\pi^+\pi^o\pi^o$	$\rightarrow K^-K^+\pi^+\pi^o$
2 $K^-\pi^+\pi^-\pi^+$ 2 D*'s	$\rightarrow K^-\pi^+e^+(\nu)$
2 $K^-\pi^+\pi^-\pi^+\pi^o$ D*	$\rightarrow K^-\pi^+\mu^+(\nu)$
$K^-\pi^+\pi^+\pi^+\pi^-\pi^-$	
2 $\bar{K}^o\pi^+\pi^-$ D*	$D^- \rightarrow K^+\pi^-e^-(\bar{\nu})$
$\bar{K}^o\pi^+\pi^-\pi^o$ D*	
$\pi^+\pi^+\pi^+\pi^-\pi^-\pi^-\pi^o$	
$K^-e^+(\nu)$	Summary
$K^-\mu^+(\nu)$	8 Λ_c
$K^-\pi^+\pi^-\mu^+\nu$	4 F
$\bar{D}^o \rightarrow K^+\pi^-\pi^o$ $\bar{D}^*$	5 charged Ds
$K^+\pi^-\pi^o\pi^o$	17 neutral Ds
$K^+\pi^-\pi^+\pi^-\pi^o$	

*** 4 Λ_c^+ are consistent with having either a Σ_c^{++} or Σ_c^o parent.
+ This event is from E564, Ammar et al., [15]

quark state) is predominantly produced at low neutrino energies. This is probably caused by the conversion of d quark to a c quark in the vicinity of the spectator u and d quarks of a d neutron. To get the charm meson production cross section from the data displayed in Figure 3 requires efficiency corrections which are not yet well known by the E531 group, but they estimate $\sigma_{charm}/\sigma_{1\mu}$ rises to $\sim 9 \pm 3\%$ at 100 GeV. The observed D^0/D^+ ratio of 2 and the $D^0 \to X\mu\nu$, $D^+ \to X\mu\nu$ branching ratios of 4% and 22%[17], respectively, imply an average branching ratio of 9.7% which would yield an opposite-sign dimuon cross section for charm of $(0.009 \pm 0.003) * \sigma_{1\mu}$. This is in good agreement with dimuon data.

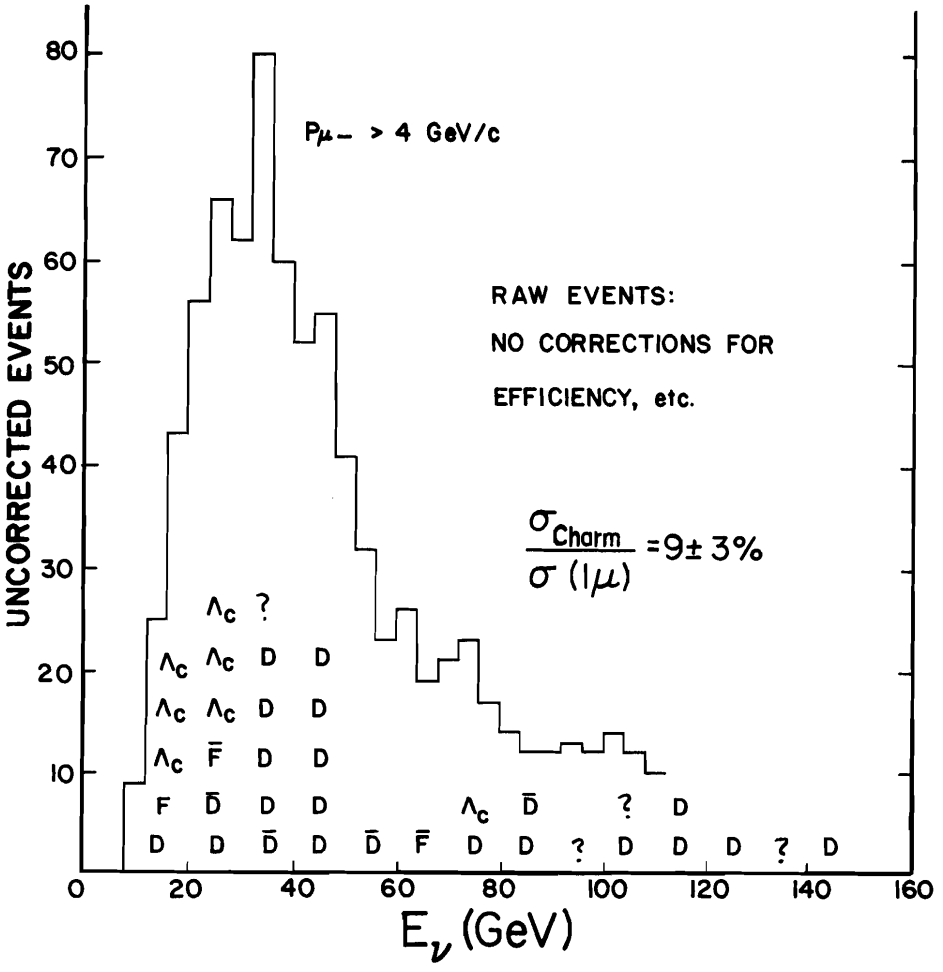

Fig. 3. E531 charm production event energy distribution. The single μ^- data require $P_{\mu^-} > 4$ GeV/c. There are no corrections for efficiency. The ambiguous data are represented by question marks. The data imply $\sigma_{charm}/\sigma_{1\mu}$ approaches 0.09 ± 0.03 at about 100 GeV.

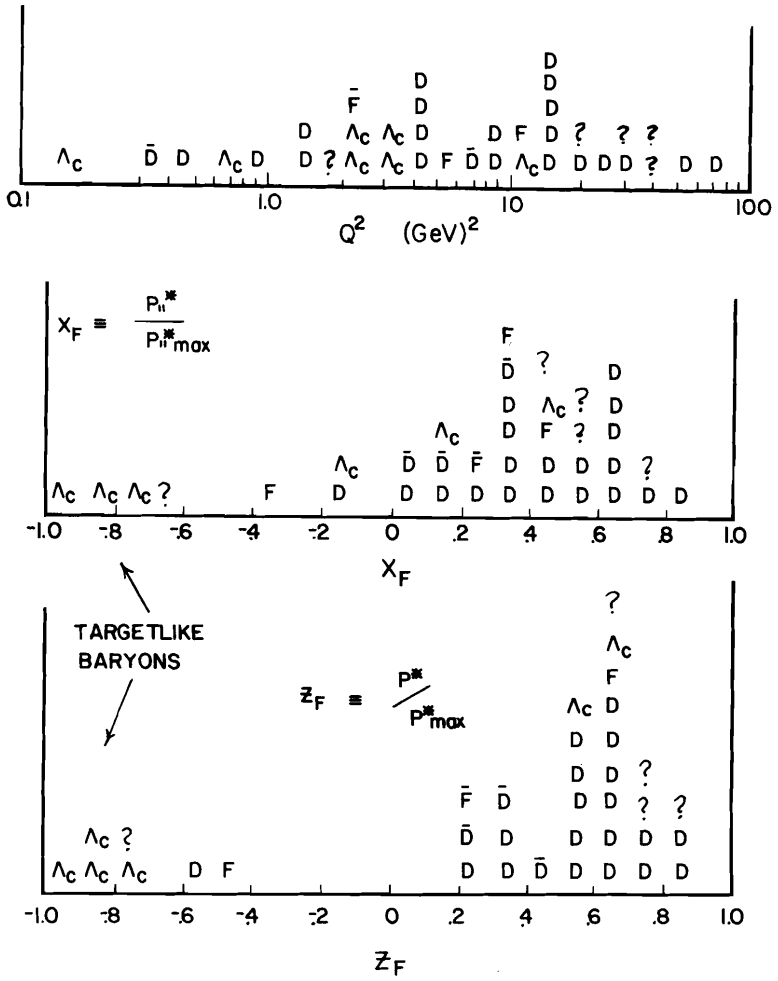

Fig. 4. E531 charm production characteristics. Note the low Q^2 for production of Λ_c and their target-like behavior. The definitions of X_F and Z_F are given in the figure.

In Figure 4 the Q^2, X_F, and Z_F distributions are given. There is only one Λ_c above a Q^2 of $4(GeV/c)^2$ and the X_F and Z_F distributions show the Λ_c is primarily target-like in its production. The W^2 vs. Q^2 correlation, not shown, reveals that the Λ_cs are generally produced at a $W^2 < 5$ GeV^2, which further suggests their target-like behavior. Thus, the charm production characteristics and estimated D cross section, relative to single muons, corroborates the previous studies of opposite sign dimuons. We can look forward to about four times as many events when the E531 experiment finishes the analysis of presently accumulated data.

III. Opposite-Sign Dimuons

A. Experimental and Theoretical Expectations

Several experiments have new data to report on charm production by neutrinos and antineutrinos. The charm events are identified by observing a second opposite-sign lepton in the final state as shown in Figure 1. The neutrino rate, $d(x)\sin^2\theta_c+s(x)\cos^2\theta_c$, has substantial contributions from both the valence down quarks and the sea strange quarks, while the antineutrino rate, $\bar{d}(x)\sin^2\theta_c+\bar{s}(x)\cos^2\theta_c$, is predominantly due to the anti-strange sea. The helicity structure, assuming V-A currents, results in the y distribution being flat, aside from the kinematics of transforming a light quark to a heavy one. This threshold effect not only changes the flat y distribution to one peaked at higher y, but also is presumed to cause the x scaling variable[18] to become $x'=x+m_c^2/(2ME_\nu y)$. This follows from the kinematics of the propagator, with four momentum q, plus x'P, where x'P refers to the momentum fraction of the initial d or s quark, which transforms to an object whose mass is m_c. The x' scaling variable then has a lower bound, $m_c^2/(2ME_\nu y)$, below which charm cannot be produced[19]. For valence quarks the charm cross section is not much affected in the low x' region, but for the strange sea distribution, $x's(x')=A(1-x')^7$, which is strongly peaked at low x', there is substantial suppression at low neutrino (antineutrino) energies[20,21]. If, in addition to the assumption of x' as the scaling variable, one includes the phase space factor (slow rescaling) for producing a heavy quark in the two body scattering:

$$\nu + \begin{bmatrix} d \\ s \end{bmatrix} \rightarrow \mu^- + c \qquad (1)$$

the charm production differential cross section becomes[19,22]:

$$\frac{d^3\sigma}{dx'dydz} = \frac{G^2ME_\nu}{\pi}\left[x'd(x')\sin^2\theta_c+x's(x')\cos^2\theta_c\right]\left[1-m_c^2/2ME_\nu x'\right] D(z) \qquad (2)$$

In equation (2) the fragmentation of the charm quark is described by the function D(z) where z is the fraction of the energy taken by the D-meson in the W-boson-nucleon center of mass.

Thus, the topics for study include fragmentation of charm, the cross section ratio $\sigma(2\mu)/\sigma(1\mu)$ as a function of energy, the 2μ neutrino and antineutrino x distributions and the fraction of strange sea in the nucleon, $\eta_s=2s/(u+d)$.

There are a number of experimental and theoretical hazards when one attempts to draw conclusions from the data.

1. In the case of the 2μ final state the second muon is identified by a minimum momentum cut of 4 to 6 GeV/c. This cut plus geometrical acceptance diminishes the charm signal by as much as 50%. For the bubble chamber μe events there is a much lower cut on the electron's momentum (typically 0.3 GeV/c) which eliminates only a small amount of charm production. However, the bubble chamber experiments suffer from a lack of statistical precision.

2. There are background second muons which result from the decay of π and K mesons originating at the hadron vertex in ordinary charged current interactions. This background is typically 5% to 20% for the dense detectors with a P_{μ_2} cut of 5 GeV/c.

3. For the wide band neutrino beam (WBB) data there is unmeasured missing energy for the decay neutrino which varies from 5 to 30 GeV and is typically 10 to 15 GeV. Thus WBB rates for $\sigma(2\mu)/\sigma(1\mu)$, are based on estimates of the missing energy.

4. The WBB antineutrino dimuon data are obtained in the presence of ~50% neutrino background. The separation of ν and $\bar{\nu}$ dimuons depends on the definition of the leading muon.

5. For the WBB data, the scaling variables, x_{vis} and y_{vis} are computed with visible energy: $E_{vis}=E_{\mu 1}+E_{\mu 2}+E_h{}^{vis}$, and $E_h=E_h{}^{vis}+E_{\mu 2}$. Consequently, they are not even on average the true x and y.

6. The fragmentation variable, z, is not measured but instead $z_{\mu_2}=p_{\mu_2}/E_h$ is the observable. In the case of the WBB data E_h does not include the energy of the decay neutrino.

7. For the counter experiments charmed baryon production is assumed to be negligible.

B. Charm Cross Sections vs. Energy

Figure 5 shows the recently published $\sigma(\mu e)/\sigma(1\mu)$ ratio versus visible energy for the Berkeley-Fermilab-Hawaii-Seattle-Wisconsin (BFHSW) 15' bubble chamber experiment[23]. The data with $P_{e^+}>0.3$ GeV/c were obtained with the quadrupole triplet beam. For comparison the 1979 Lepton-Photon conference data from the Columbia-BNL[1,24] and Gargamelle-SPS[25] 2μ (corrected for efficiency) experiments are shown. By 100 GeV the charm production has

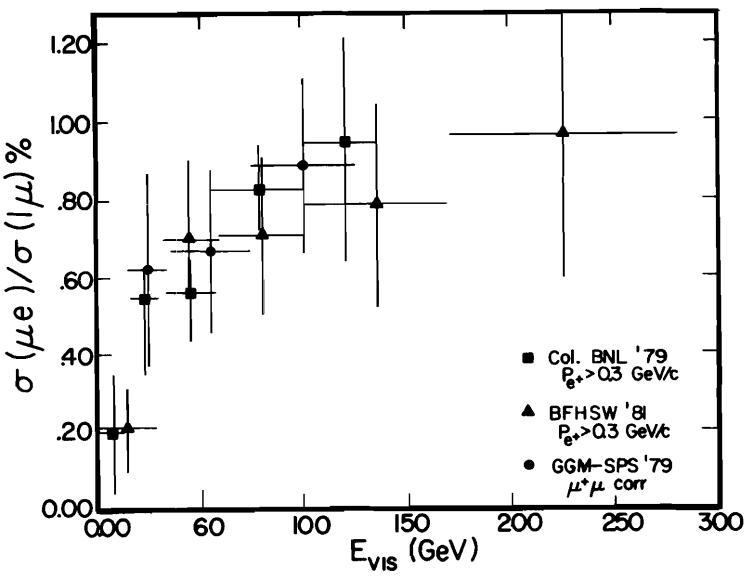

Fig. 5. $\sigma(\mu e)/\sigma(1\mu)$ vs E_{vis}. The data are from references 23, 24, 25. The positron momentum cut requires $P_{e^+} > 0.3$ GeV/c. The GGM-SPS $\mu^-\mu^+$ data shown here are corrected. See Ref. 25.

risen to 0.85% of the single muon cross section. Figure 6 shows the same Columbia-BNL and BFHSW μe data with a 4 GeV cut on the e^+. New 2μ data from the CHARM collaboration are also shown with a 4 GeV/c cut on $P_{\mu 2}$(495 events)[26]. The CHARM data are obtained with the WBB. Their detector has an average density of 1.3 gm/cm^3 as compared to the CDHS, CFRR, and HPWF detector densities of 5.18, 4.02 and 4.51 gm/cm^3. Instead of making a background subtraction, the CHARM collaboration uses the observed distribution of the distance between the two muons at the vertex to deduce the fraction, f, of the dimuon signal which is prompt. They find $f_\nu = 0.62 \pm 0.04$ and $f_{\bar{\nu}} = 0.58 \pm .06$. For neutrinos the agreement in $2\mu/1\mu$ rates is reasonable although the CHARM data seem to be systematically lower than the bubble chamber data.

CDHS and CFRR also report new neutrino and antineutrino dimuon data. The CDHS WBB ν data come from 15,000 dimuon events while the CFRR ν data consists of 484 events obtained with the Fermilab dichromatic narrow-band

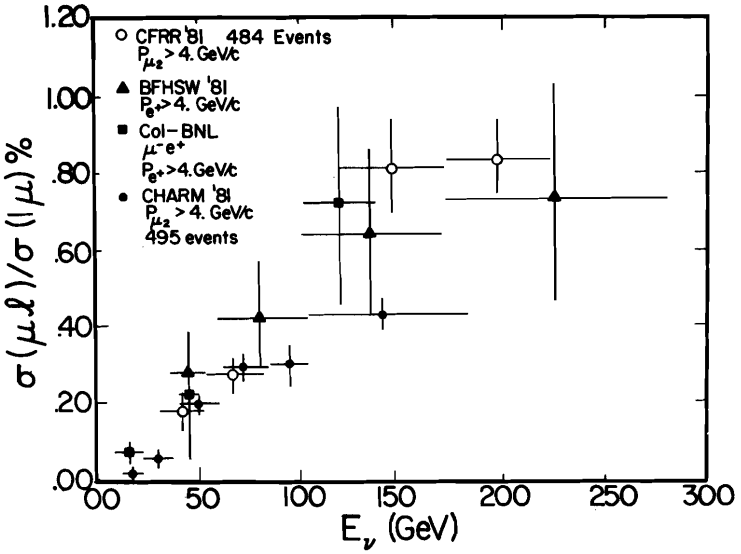

Fig. 6. $\sigma(\mu\ell)/\sigma(1\mu)$ vs E_{vis}. The momentum cut on the second lepton is 4 GeV/c. The data shown are from those in Fig. 5 and also from the CHARM collaboration[26].

beam (NBB). Figure 7 shows the CFRR visible energy versus radius of the interaction for the ν dimuon events. Clearly the separation of K and π neutrino events is straight forward. For the CFRR NBB data the total energy for each event is assigned from a cross section weighted average of the neutrino flux at that radius. The CFRR data, with $P_{\mu 2} > 4$ GeV/c are shown in Figure 6. CDHS have used their NBB 2μ events and Monte Carlo calculations to correct for the missing energy in their WBB data and to obtain the $2\mu/1\mu$ cross section ratio versus neutrino energy (not E_{vis}). For the CDHS data the second muon is identified by its passage through 5 modules of their apparatus. This implies a $P_{\mu 2}$ cut which varies between 5 and 6.5 GeV/c. The CDHS and CFRR data, with a 6.5 GeV/c $P_{\mu 2}$ cut on the CFRR data, are shown in Figure 8. The data show reasonable agreement. Both sets of data have the K and π decay background subtracted. For CFRR the 2μ background/1μ rate varies approximately linearly with energy and reaches 0.6×10^{-4} at $E_\nu = 200$ GeV. CDHS have corrected their data for acceptance and the $P_{\mu 2}$ cut with a Monte Carlo which assumes a fragmentation function $D(z) = \text{constant}$ and no slow rescaling. These corrected (preliminary) data are shown in Figure 9. Again as was seen in Figure 5, the $2\mu/1\mu$ cross section rises to ~1% for $E_\nu > 100$ GeV. Figure 9 also shows the CDHS antineutrino $\mu^+\mu^-$ cross section data with the π and K decay background subtracted and corrected as in the case of neutrinos.

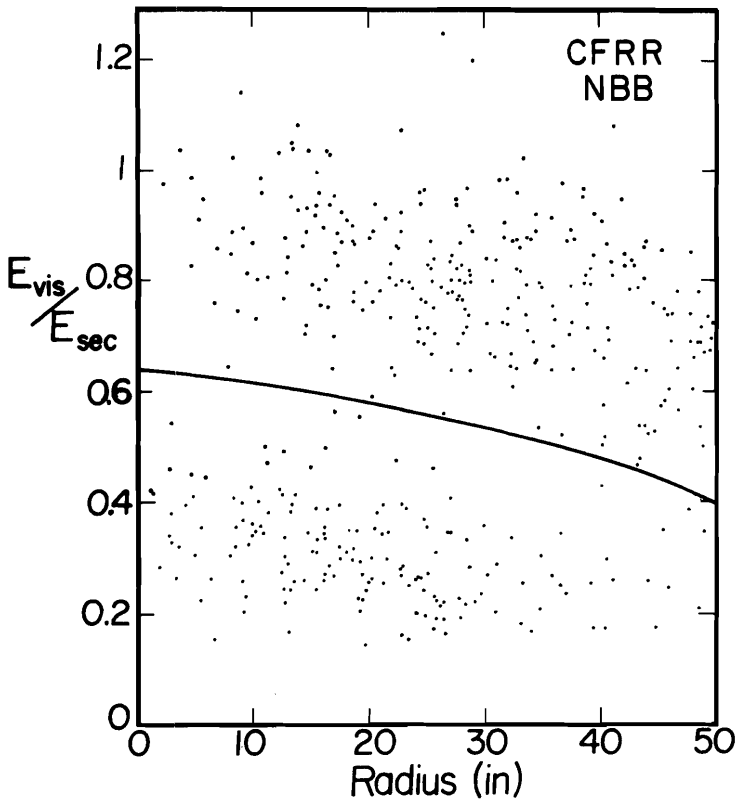

Fig. 7. E_{vis}/E_{sec} vs. R_{int} for the CFRR opposite sign dimuons. The scaled energy vs. radius of the interaction point clearly shows the ν_K, ν_π separation. The curve is the boundary used in the separation.

A comparison of the CDHS corrected neutrino and antineutrino data show the $\bar{\nu}$ data exceed the ν data at all energies. The shape of the cross section rise has not yet been fitted to the slow rescaling hypothesis. Edwards' and Gottschalk's slow rescaling calculation[21] indicate the ratio $(\sigma_{2\mu}^{\bar{\nu}}/\sigma_{1\mu}^{\bar{\nu}})/(\sigma_{2\mu}^{\nu}/\sigma_{1\mu}^{\nu})$ rises from zero at low energy to approximately one at 50 GeV and then increases slightly above this energy. Exactly where the $\bar{\nu}$ ratio overtakes the ν ratio depends sensitively on the parameters involved in the slow rescaling calculation, namely the shapes of the valence and strange sea x distributions, the charmed quark mass, and the fraction of strange sea in the nucleon.

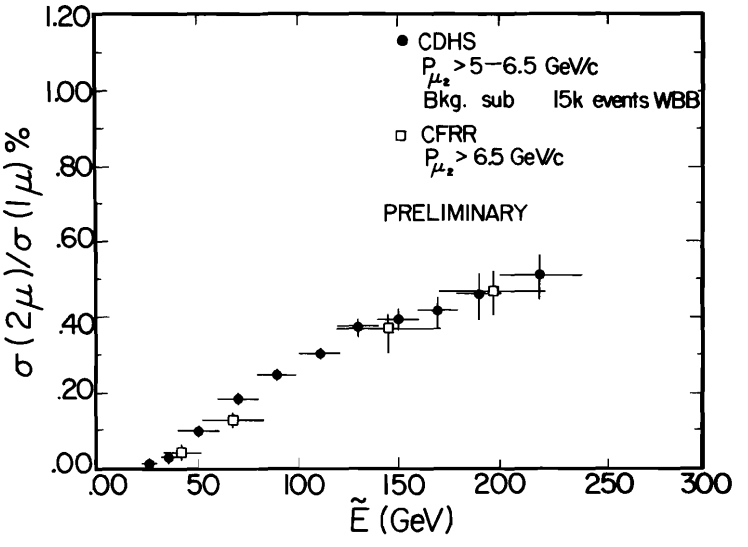

Fig. 8. Comparison of the CDHS and CFRR ratio $\sigma(\mu^-\mu^+)/\sigma(\mu^-)$ vs. neutrino energy. The CDHS data are from Ref. 27.

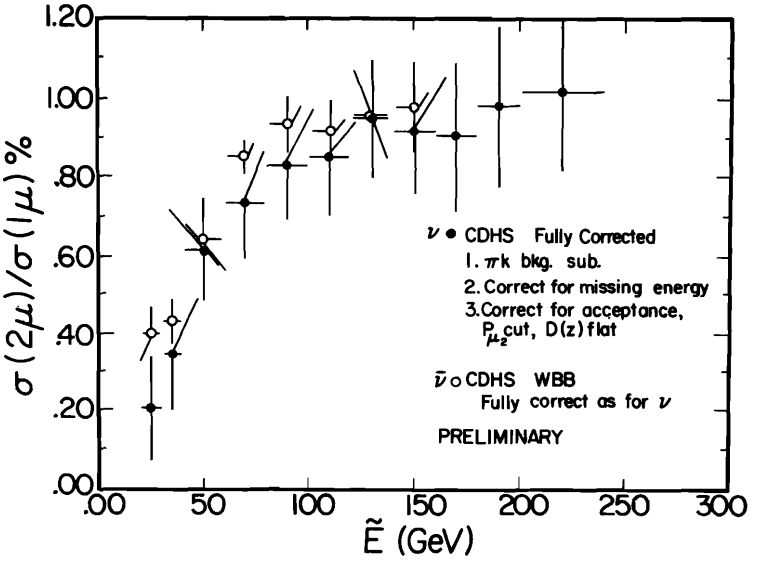

Fig. 9. Neutrino and antineutrino 2μ/1μ cross section ratios vs. neutrino energy. The data are from Ref. 27.

C. x Distributions

Although the scaling variable, x', is expected to be fundamentally related to the parton density distribution, there are good reasons for studying x distributions[21]. The x' distribution has a threshold in the small x' region which varies with neutrino energy E_ν, inelasticity y, and the assumed charmed quark mass, m_c. Furthermore the effects of apparatus acceptance and resolutions ($\Delta E_h/E_h$, $\Delta\theta_\mu/\theta_\mu$, etc.) complicate the study of the variable x'. Thus experimenters have reported x, rather than x' distributions. Edwards and Gottschalk show expected experimental x distributions for various theoretical x'd(x') and x's(x') distributions, and they also point out the need to include experimental resolution effects in these predictions. The CFRR observed x distribution has been corrected for $P_{\mu 2}$ and acceptance cuts. If the fragmentation function, D(z), is assumed to be a constant, the CFRR x distribution weighting function, with a $P_{\mu 2}$ cut of 4 GeV, increases almost linearly by about 30% over

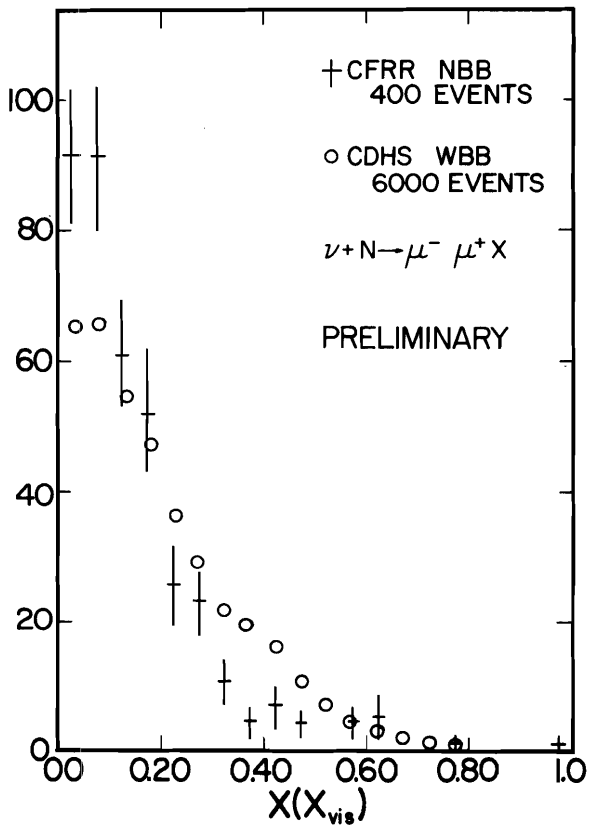

Fig. 10. Opposite-sign neutrino dimuon x distributions. For the CDHS data (Ref. 27) x_{vis} is plotted.

the x range from 0 to 0.6 at a neutrino energy of 100 GeV. For CDHS the detection efficiency is uniform so that no correction has been applied to their x distributions.

The neutrino x distributions for CDHS and CFRR are shown in Figure 10. For CDHS the calculated quantity is x_{vis} which is usually about 0.01 larger than the true x due to missing energy. The $\langle x \rangle$ for the CFRR data is 0.15 ± 0.02, while CDHS measure $\langle x_{vis} \rangle$ to be 0.195 ± 0.01. CHARM reports an $\langle x_{vis} \rangle$ of 0.21 ± 0.01. Beside the expected small difference between $\langle x \rangle$ and $\langle x_{vis} \rangle$ due to missing energy, some additional difference is anticipated because of the different average Q^2. It should be emphasized that the data analysis of both CDHS and CFRR experiments is incomplete and that the different 1^{μ} average energies of 60 and 100 GeV, respectively for CDHS and CFRR, and the different muon angular resolutions may account for the difference in mean x.

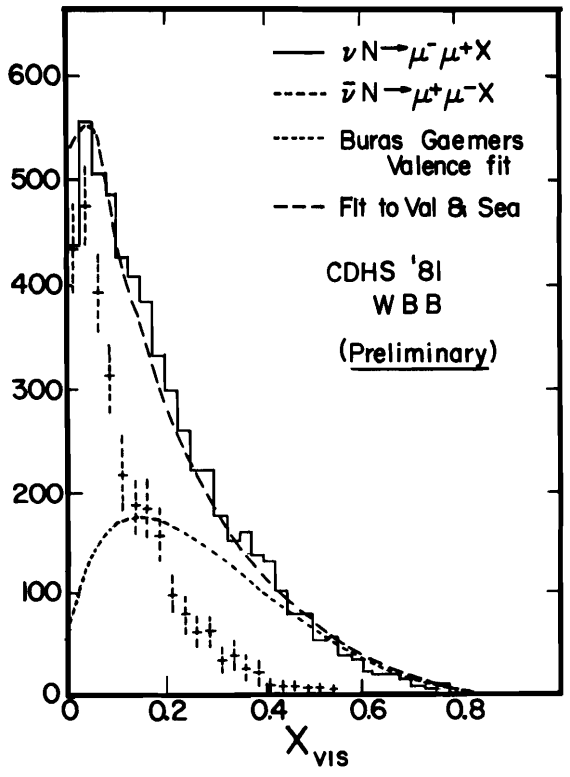

Fig. 11. CDHS neutrino and antineutrino x distributions. Ref. 27.

For antineutrinos the CDHS x distribution shown in Figure 11 can be fitted with $x\bar{s}(x)=A(1-x)^7$. This form is also consistent with the new CFRR $\bar{\nu}$

data and other older data. The value of $\langle x_{vis} \rangle$ for the CDHS $\bar{\nu}$ data is 0.095±0.01 while CHARM finds 0.15±0.01. These smaller values of $\langle x_{vis} \rangle$ are expected since nearly all of the $\bar{\nu}$ charm events are produced from the strange sea.

D. Strange Sea Content of the Nucleon

Two methods have been used to extract the strange sea content of the nucleon:

$$\eta_s \equiv \frac{2 \int x\, s(x)\, dx}{\int x[u(x) + d(x)]dx} .$$

In the first method the neutrino dimuon x distribution is fitted using the valence x distributions, u(x) and d(x), from standard deep inelastic scattering and the strange sea, s(x), taken from the x distribution of opposite-sign antineutrino dimuons. Thus the relative strength of the strange sea is determined from fitting α in the equation:

$$\frac{dN_{\mu\mu}}{dx} = (1-\alpha) \times d(x) + \alpha\, xs(x) .$$

The second or double ratio method uses the ratios of integrated rates for one and two muons (neglecting charmed baryon production):

$$R_1 \equiv \sigma_{\bar{\nu}}(1\mu)/\sigma_{\nu}(1\mu) ,$$

$$R_2 \equiv \frac{\sigma_{\nu}(2\mu)/\sigma_{\nu}(1\mu)}{\sigma_{\bar{\nu}}(2\mu)/\sigma_{\bar{\nu}}(1\mu)} ,$$

and

$$\eta \equiv \frac{\int [\bar{u}(x) + \bar{d}(x)] \times dx}{\int [u(x) + d(x)] \times dx} \approx 0.15,$$

to find:

$$R_2 = R_1 \frac{\sin^2\theta_c + \eta_s \cos^2\theta_c}{\eta \sin^2\theta_c + \eta_s \cos^2\theta_c} ,$$

which yields:

$$\eta_s = \frac{\tan^2\theta_c\, (1 - \eta\, R_2/R_1)}{(R_2/R_1 - 1)} .$$

Both methods have been used by CDHS to find η_s. In Figure 11 the CDHS x distributions are shown, summed over all energies, along with the fitted curves, and Figure 12 shows the CDHS values of η_s, without slow rescaling, for both methods as a function of neutrino energy. The average value for η_s, not including systematic errors, for the CDHS data is 4.6±0.6%. CFRR

and CHARM report preliminary average values without slow rescaling of $3.9\pm1.0\%$ and $5.0\pm1.5\%$, respectively. While slow rescaling raises the value[20,21] of η_s, preliminary results from CDHS which include slow rescaling suggest that $\eta_s=\eta$, i.e. the strange sea may not be SU(3)-symmetric.

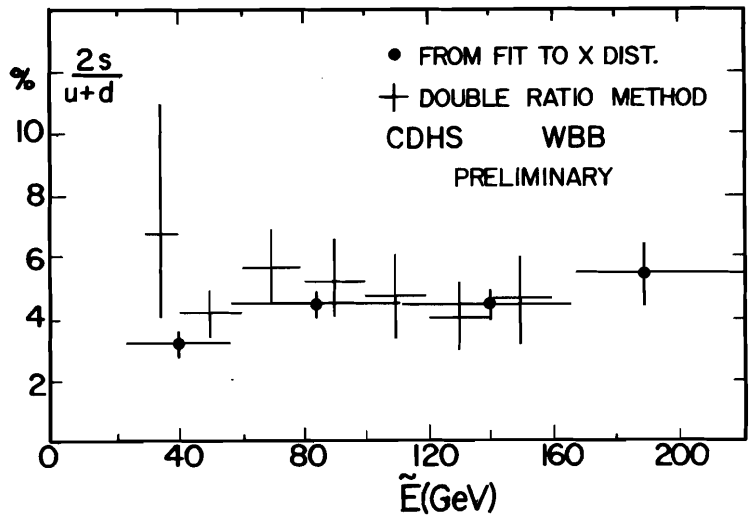

Fig. 12. Strange sea content of the nucleon. The CDHS results of both the fits to the x distributions and the double ratio method are shown. No slow rescaling has been included in the fits (Ref. 27).

IV. Like-Sign Dimuons

A. Old Data and Possible Sources

In the past, several groups have reported like-sign rates statistically well above their measured and/or calculated background rates. Figure 13 shows the $\nu N\to\mu^-\mu^- x$ cross section ratios as reported[28-32] before 1981. All groups agree that the second muon originates at the hadron vertex. This conclusion follows from the fact that the ϕ distribution is peaked at 180°, where ϕ is the angle between the two muon tracks projected on a plane perpendicular to the incident neutrino. Mechanisms which have been suggested as prompt sources for these signals include (1) associated charm production, (2) b(bottom) meson or baryon production, and (3) D°, $\bar{D}^\circ$ mixing.

The associated production model[33] which describes first order QCD gluon bremsstrahlung into $c\bar{c}$ pairs, Figure 14a, predicts a like-sign rate smaller by one or two orders of magnitude than the experimental rates (see Figure 13). Theoretical predictions for hadronic production of bare charm pairs by gluon bremsstrahlung are also lower than the observed rate by roughly the same amount.

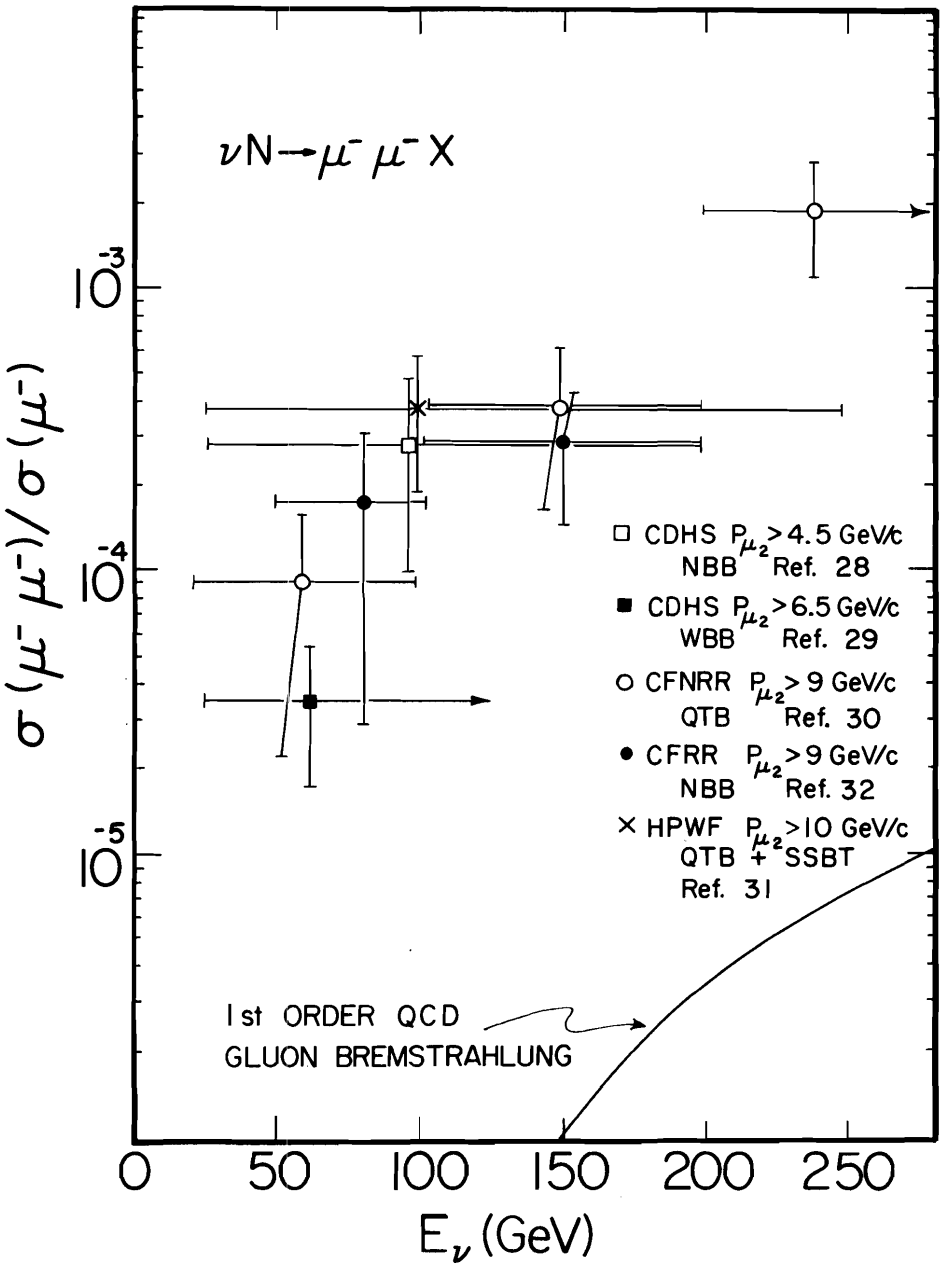

Fig. 13. Like-sign neutrino dimuon rates vs. E_ν for data available before 1981. The curve is the predicted rate for $c\bar{c}$ pair production by gluon bremstrahlung with the requirement of $P_{\mu_2}>9$ GeV.

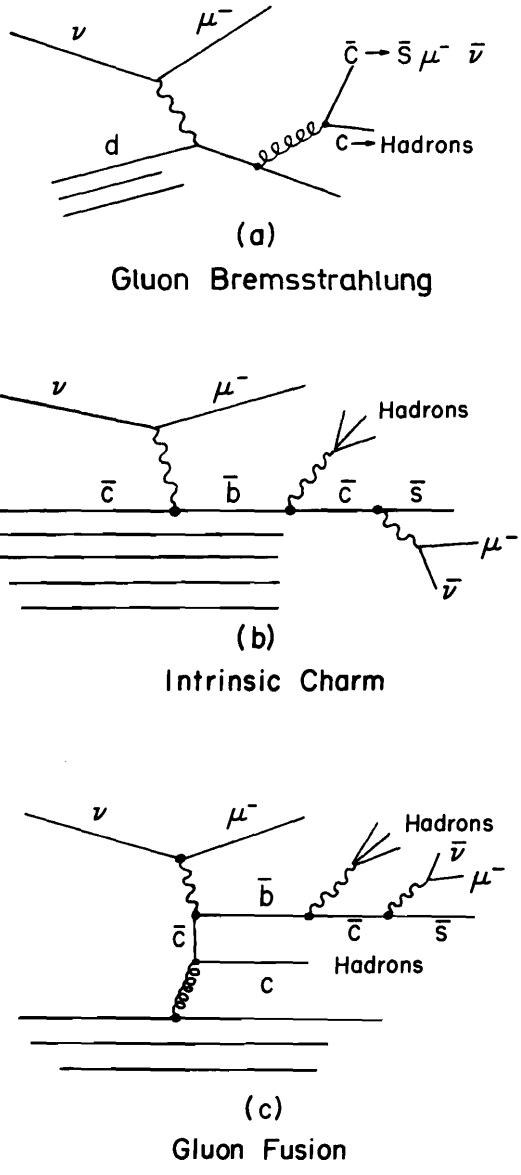

Fig. 14. Possible models for production of like-sign dimuons. For associated charm production, (a), see Reference 33. For b production models, (b) and (c) see References 34 and 36.

As an example of b production, Brodsky, Peterson, and Sakai[34] (BPS) proposed intrinsic charm in the nucleon, Figure 14b, to explain the observed like sign ν rates as well as the large diffractive cross section observed in $pp \rightarrow \Lambda_c^+$ at the ISR[35]. With the assumption of 1% intrinsic charm and the requirement of $P_{\mu_2} > 9$ GeV/c their model fails to give enough rate because the (V-A) coupling of c to b quarks requires a $(1-y)^2$ factor in the cross section, which severly limits b quark production. BPS point out that the mean value of x expected in the intrinsic charm model would be larger than is the case for gluon bremsstrahlung since the c and $\bar{c}$ have significantly larger mass than the u and d quarks, therefore carrying a larger fraction of the nucleon's momentum.

Another b production model which has been investigated by Barger, Keung and Phillips[36] is gluon fusion as shown in Figure 14c. They find the cross section for this process to be even smaller than the intrinsic charm model and conclude that of the three models discussed the only one that comes close to the data is intrinsic charm with full strength right-handed coupling. If the rate is to be explained with left handed (V-A) coupling, the intrinsic charm would have to account for a much larger fraction of the nucleon's momentum and this would be inconsistent with the large-x dimuon cross section observed in muon scattering by the EMC group (see the report by Strovink in these Proceedings).

D^o, $\bar{D}^o$ mixing should be considered as a possible source of like-sign events. Although there is no evidence for mixing and theoretical prejudice suggests a rate of $\sim 10^{-3}$ or less, the measured mixing at 90% confidence limit is less than 11% (Avery et al.[37]) and less than 16% (95% CL, Feldman et al.[38]). If, for example, all the like-sign dimuons in the CFRR experiment came from D^o, $\bar{D}^o$ mixing (which is unlikely because one would expect associated charm production at some level) the D^o/D^+ production ratio plus $D \rightarrow \mu$ inclusive branching ratios discussed in II-C above would imply D^o, $\bar{D}^o$ mixing at more than the 20% level. This level would be difficult to satisfy with the existing D^o and D^+ production and branching ratios, but it is possible a fraction of the like-sign signal comes from this source. There is some evidence D^o, $\bar{D}^o$ mixing is smaller than the limits quoted here[39]. If so, the fraction of like-sign events due to mixing would be small.

B. Background Calculations

The expected background sources of like-sign dimuons are: (1) decay of a primary π or K at the hadron vertex in ordinary 1μ charged current interactions, and (2) the production of either a prompt or non-prompt second muon from the interaction of the primary hadrons in the hadron shower. Sufficient data are available to reliably calculate both of these contributions to the like-sign rate.

The rate from decays of the primary hadrons is calculated in two ways. The first approach is to generate the inclusive primary hadron spectra and multiplicity from Field-Feynman quark jets based on fits to νNe data obtained with the WBB. An alternative, and perhaps better procedure is to take the measured inclusive hadron spectra from high energy νNe bubble chamber data. The secondary particle cascade calculation makes use of the generated or measured primary hadrons, as just described, along with the measured prompt and non-prompt μ production by hadrons in the Fermilab experiment E379/595 variable density target. This gives the rate as a function of hadron energy, E_H, for producing a muon with momentum greater than some cutoff value, P_{μ_2}. Figure 15 shows an example of such a calculation by the CFRR group [32]. The number of like-sign background 2^{μ} events is then obtained by convoluting this probability curve with the experimentally measured hadron energy distribution for the 1^{μ} event sample. A comparison of the CFRR calculation with that of CDHS shows the CFRR curve

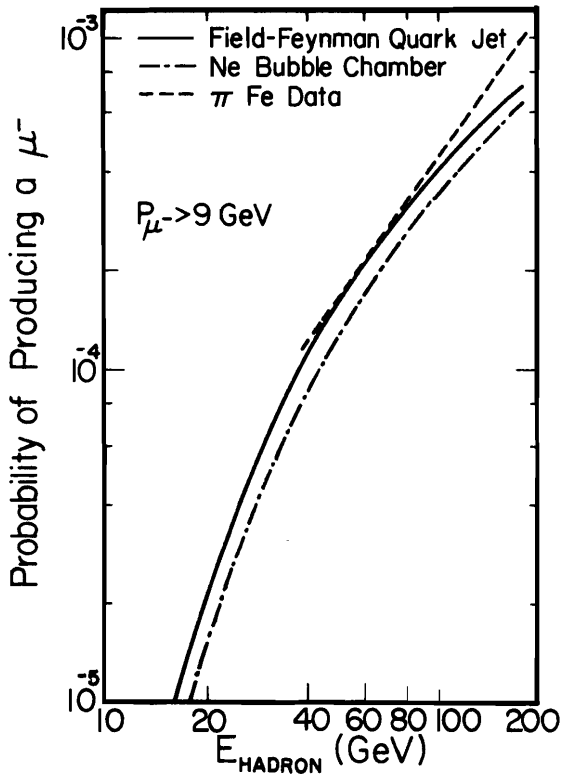

Fig. 15. Probability of producing a μ^- with momentum greater than 9 GeV/c given hadron energy, E_H, from pions and kaons. The solid curve uses the Field-Feynman quark jet program; the dot-dashed curve uses ν-Ne bubble chamber data directly. The solid curve is production by incident pions.

to be about 25% higher than CDHS for a $P_{\mu 2}$ cut of 9 GeV/c. Although the CDHS and CFRR background calculations give similar rates, there are differences in the way the curves are used since the two detectors differ. The CFRR experiment demands a muon in the spectrometer downstream of its target calorimeter which in turn requires the hadron shower to point in a direction that allows the second muon to enter the toroid. In addition, since the leading muon is required to enter the toroid, the largest y region (largest E_H), where the probability for producing a decay muon is greatest, does not contribute to the background. These factors reduce the number of background second muons for CFRR by a factor of two to three.

C. New Data

CDHS[27], CHARM[26], and HPWFOR[40] all have reported new data on like-sign dimuons. The CHARM and HPWFOR experiments have determined their backgrounds in ways which differ from the calculations discussed above. As mentioned in the section on opposite sign dimuons, the CHARM collaboration 2μ tracks which emerge from the hadron shower are projected back to the event vertex to find the horizontal and vertical distances which separate the two muons. The histogram of projected distance is used to extract the prompt fraction of like sign dimuons. They first take each of their 2μ events and computer generate an event in which the two muons originate at the same vertex. Each muon is then given the multiple scattering appropriate to its measured momentum and the newly generated event is analyzed as a normal 2μ event to obtain the perpendicular vertex distribution ($\Delta y, \Delta z$) for prompt events. To find the vertex resolution function for muons from hadron decay, they use 891 hadrons which emerge from the hadron shower, go through 12 modules without showering, and then interact. This gives the correct sample as to hadron energy, angle, etc. for calculating a decay background distribution. The $P_{\mu 2}$ cut they apply to their data is 4 GeV/c, which makes it difficult to compare their results with the other three counter experiments which have a $P_{\mu 2}$ cut of 9 or 10 GeV/c.

The HPWFOR group use their neutrino-induced opposite sign dimuons to establish the slope of the $\mu^-\mu^+/\mu^-$ rate versus absorption length since they have a target with three different densities. The fixed slope, which agrees with their background calculations, is then used with their like sign data to establish the prompt rate.

The new and old data are shown in Figure 16. The new CHARM and 1979 CDHS data require $P_{\mu 2} > 4$ and 6.5 GeV/c, respectively. Thus, an appropriate comparison of those data with all the other data, which require $P_{\mu 2} > 9$ GeV/c, is difficult. The CFRR and HPWFOR data taken with the quadrupole triplet beam (QTB) and NBB seem to be in reasonable agreement. However, those data, QTB+NBB, are in poor agreement with the CERN WBB data. There are several places to look for difficulties, particularly since the background subtractions are different for each experiment.

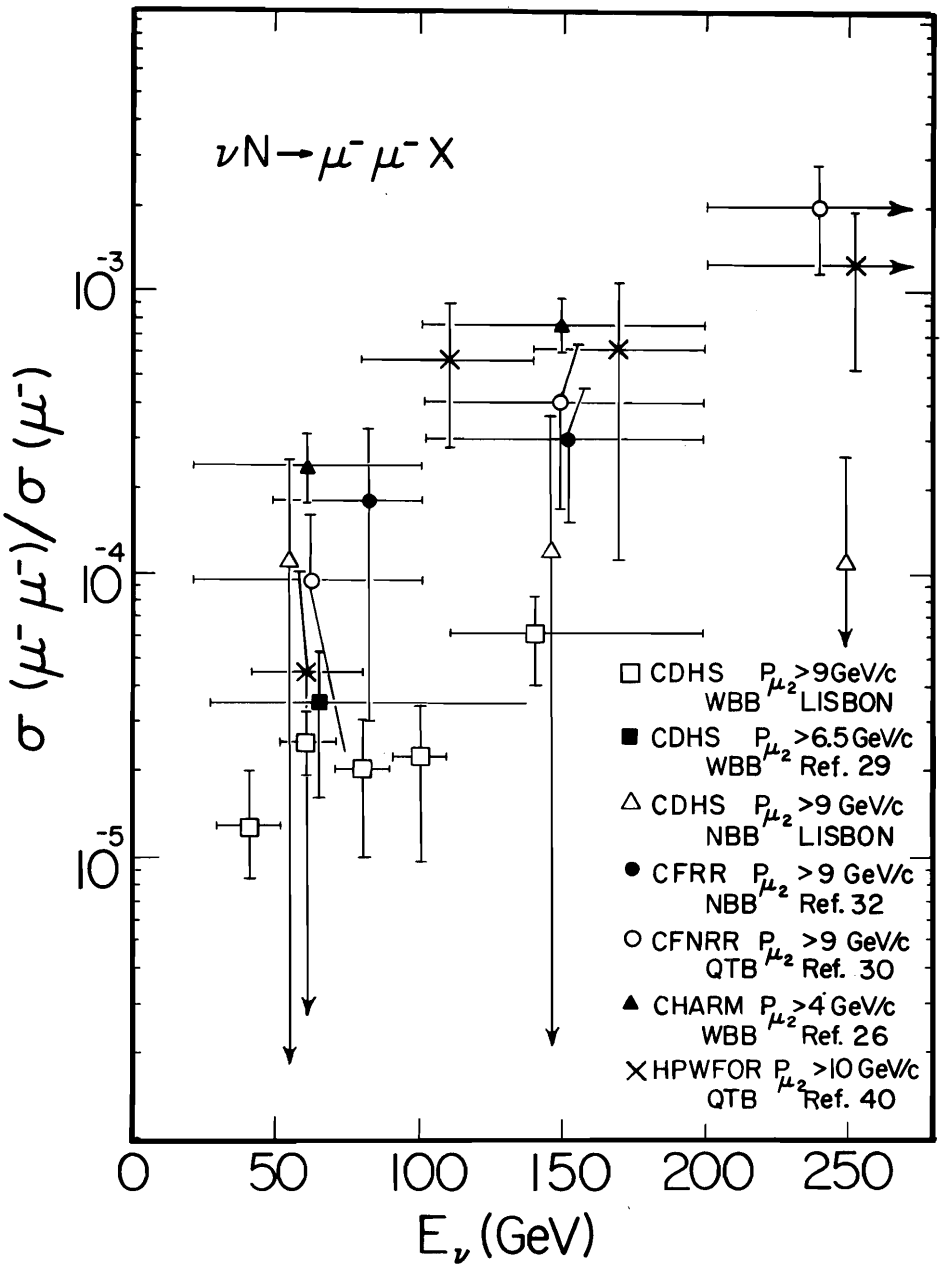

Fig. 16. Neutrino like-sign dimuon rates vs. E_ν.

For the three detectors which have similar densities, CDHS, CFRR, and HPWFOR, the fractions of the 2μ data that are estimated to be background are roughly 65%, 30%, and 25%, respectively. CFRR and HPWFOR have similar detectors and similar geometrical requirements which account for their smaller background estimates than CDHS. The raw rates for the experiments should differ only because their average densities differ. The raw rates for CDHS and CFRR at 150 GeV are (1.63±0.18 and 4.2±1.3) x 10^{-4} while the absorption lengths for these detectors are 28 and 36 cm, respectively. Assuming the total CDHS raw rate were background, this would imply a rate for the CFRR density of (36/28)*1.63=2.1±0.2 in units of 10^{-4} which is in poor agreement with the measured rate. If such a difference existed at only a single energy it would be argued that the statistics of disagreement were not overwhelming, but the difference exists throughout the energy range 50 to 250 GeV. The agreement of raw rates is, at best, poor. The CHARM and HPWFOR raw rates are not available to help sort out this problem. CHARM has not yet stated a raw rate with P_{μ_2}>9 GeV and HPWFOR have only a combined raw rate for their two lowest densities (iron calorimeter and liquid scintillator target) since the energy is not determined for their high density iron target events.

There is at least one significant difference in calculating the NBB and WBB $\mu^-\mu^-/\mu^-$ data rates. For the NBB data the number of 1μ events used in the denominator is easily determined since the $\mu^\pm\mu^\pm$ event energy and vertex radius identifies whether the event came from a ν_π or ν_K interaction. On the other hand from Figure 17, which shows both the QTB and WBB 1μ E_ν spectra, one observes the rapid decrease in events with energy for the WBB. Since there is missing energy in the 2μ events, the number of 1μ events to use in the denominator must have a mean energy which is higher than the 2μ average, E_{vis}. For example, taking the mean missing energy of 13 GeV in the 150 GeV $\mu^+\mu^-$ CFRR NBB data to be the same as the missing energy in the WBB $\mu^-\mu^-$ data would raise the raw WBB $\mu^-\mu^-/\mu^-$ rate by about 50%. Furthermore, the WBB background subtraction would be smaller since it is based on the number of 1μ events. Since the $\mu^-\mu^-$ prompt source is not known, it is difficult for the WBB experiment to estimate what the missing energy correction should be. CDHS and CHARM make no mention of correction for missing energy in their measurement of like-sign rates. Similar criticism can be leveled at the QTB experiments, although the energy spectrum falls off much less rapidly over the energy region of interest.

The FIIM $\bar{\nu}$ bubble chamber experiment[41] reports 4 μ^+e^+ events when a background of 1.1 events is expected. This leads to a like-sign rate of $4.8^{+5.3}_{-3.2}$x10^{-4} with the average μ^+e^+ event energy of 52 GeV. The BFHSW group[23] also reports 3 μ^-e^- events and 1 μ^+e^+ with estimated backgrounds of 3.6 and 0.3 events. Although the rate for one μ^+e^+ is consistent with background calculations, the observed e^+ momentum of 6.6 GeV/c makes the event a very unlikely candidate for production by K and π decay. There are

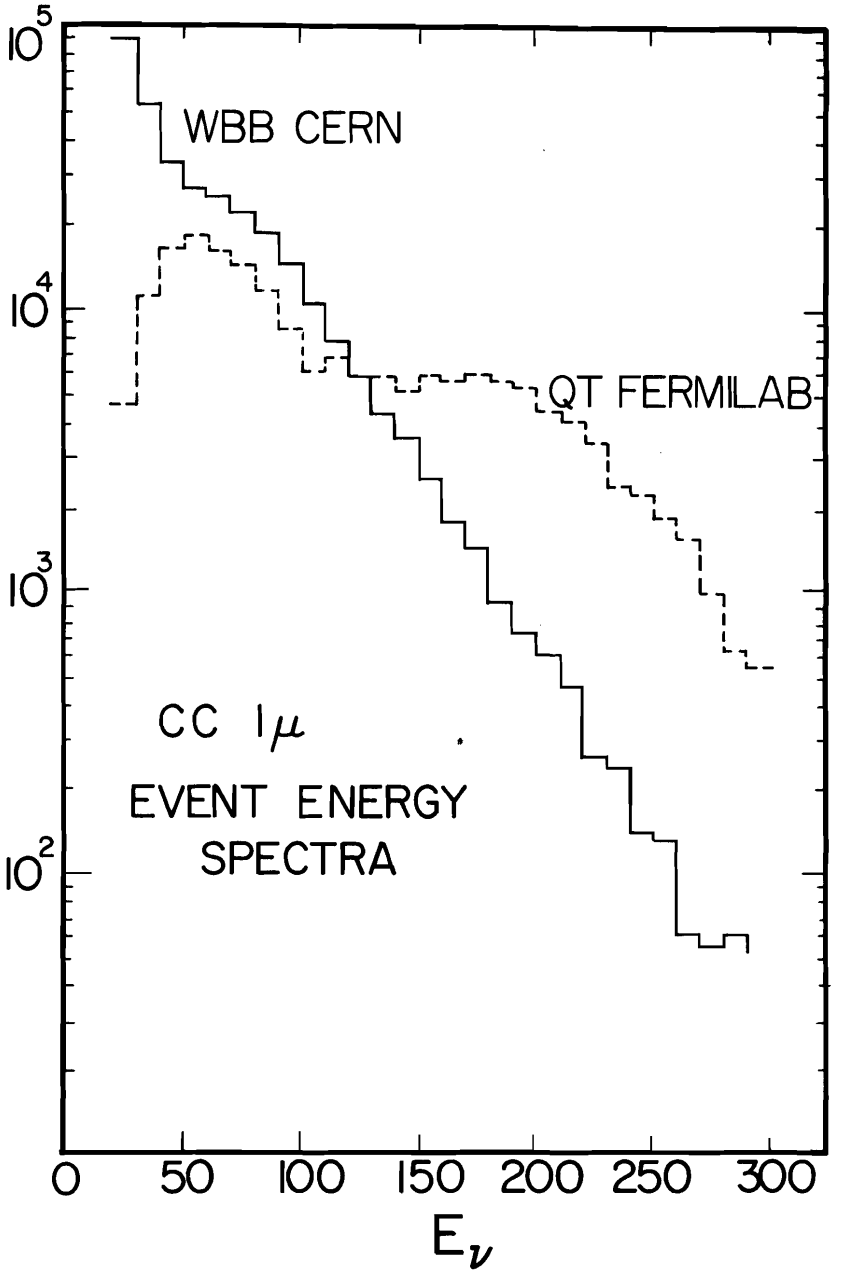

Fig. 17. Neutrino charged current single muon energy spectra for the CERN wide band beam and Fermilab quadrupole triplet beam.

no new Columbia-BNL like-sign data since the 1979 Lepton-Photon conference at which they reported 20 μ^-e^- events with an expected background of 9 events giving a $\mu^-\mu^-/\mu^-$ rate $\sim 3\times10^{-4}$.

V. Conclusions

A. Charm Production

1. Charmed baryons are produced at $W<5$ GeV and at low Q^2. Usually they appear as target-like fragments.

2. For $E_\nu > 30$ GeV charm production is almost entirely F and D mesons or their excited states.

3. The charm production cross section for neutrinos is 8% to 10% of the 1 μ cross section for neutrino energies above 100 GeV.

4. Although the rise in the charm production cross section with energy is consistent with calculations based on the idea of slow rescaling, there is not yet a test which unequivocally proves that the quarks have mass and that the mass effects are present in x distributions.

5. The strange sea momentum fraction, without rescaling is ~5%. It would be higher with slow rescaling although it is doubtful the strange sea is SU(3) symmetric ($\bar{u}=\bar{d}=s=\bar{s}$). The value of η_S and its x and Q^2 dependence is important in its own right and it also plays a vital role in comparing structure functions obtained with muons and neutrinos.

B. Like-Sign Data

1. All experiments report like-sign dimuon signals, substantially above backgrounds but they do not all agree on the level. Data from the narrow band and quadrupole triplet beams exhibit higher rates than from the wide band beams. A non-negligible part of the difference between rates may be due to missing energy, which cannot be determined for wide band beam data.

2. Even the lowest measured rates are larger than the calculated rate for the associated production of charm pairs via gluon bremsstrahlung or b-quark production from (V-A) coupled models based on (a) intrinsic charm in the nucleon or (b) gluon-fusion.

3. If the like-sign signal were due to D^0, $\bar{D}^0$ mixing, the required level of mixing would be larger than measurements indicate. Thus, mixing could account for only a fraction of the observed rate if our knowledge of D^+, D^0 production and branching ratios is accurate.

VI Acknowledgements

The author would like to thank the experimental groups whose work appears here, for access to their data before publication. I would like to acknowledge the help of W. Reay and R. Sidwell of E531, K. Kleinknecht, B. Peyaud, aud R. Turlay of CDHS, U. Amaldi, A. Capone, and K. Winter of CHARM, R. Imlay and T.Y. Ling of HPWFOR, and especially my own collegues of CFRR[42] for help in preparing this report.

VII References

1. M.J. Murtagh, Proceedings of the 1979 International Symposium on Lepton and Photon Interactions at High Energies, edited by T.B.W. Kirk and H.D.I. Abarbanel (Fermilab, Illinois, 1979), p. 277.
2. J.D. Bjorken, and S. Glashow, Phys. Lett. 11, 255 (1964). S. Glashow, J. Illiopoulos, and L. Maiani, Phys. Rev. D2, 1285 (1970).
3. G. Altarelli, et al., Phys. Lett. 48B, 435 (1974).
   M.K. Gaillard, Conference Proceedings: Neutrino-74, C. Baltay -editor, p. 65 (1974); For review see M.K. Gaillard, B.W. Lee, and J.L. Rosner, Rev. Mod. Phys. 47, 277 (1975).
4. M. Kobayashi and K. Maskawa, Progr. Theor. Phys. 49, 652 (1973).
5. E.G. Cazzoli et al., Phys. Rev. Lett. 34, 1125 (1975).
6. E.H.S. Burhop et al., Phys. Lett. 65B, 299 (1976).
7. C. Baltay et al., Phys. Rev. Lett. 41, 73 (1978).
8. A.M. Cnops et al., Phys. Rev. Lett. 42, 197 (1979).
9. C. Baltay et al., Phys. Rev. Lett. 42, 1721 (1979).
10. J.D. Prentice, Proceedings of the 1979 International Symposium on Lepton and Photon Interactions at High Energies, edited by T.B.W. Kirk and H.D.I. Abarbanel (Fermilab, Illinois 1979) p. 563.
    N. Ushida et al., Phys. Rev. Lett. 45, 1049 (1980).
    N. Ushida et al., Phys. Rev. Lett. 45, 1053 (1980).
11. One of the D^0 candidates is discussed in reference 6 above.
    C. Angelini et al., Phys. Lett. 84B, 150 (1979).
12. H. Grässler et al., Phys. Lett. 99B, 159 (1979).
    J. Blietschau et al., Phys. Lett. 86B, 108 (1979).
13. T. Kitagaki et al., contributed paper 9. 1981 International Symposium on Lepton and Photon Interactions at High Energies (Bonn, Aug. 24-29, 1981).
14. N. Stanton, Proceedings of the 1981 Hawaii Conference.
15. R. Ammar et al., Phys. Lett. 94B, 118 (1980).
16. V. Luth, Proceedings of the 1979 International Symposium on Lepton and Photon Interactions at High Energies, edited by T.B.W. Kirk and H.D.I. Abarbanel (Fermilab, Illinois, 1979) p. 78.

17. W. Bacino et al., Phys. Rev. Lett. 45, 329 (1980).

18. R.M. Barnett, Phys. Rev. Lett. 36, 1163 (1976).

19. J. Kaplan and F. Martin, Nucl. Phys. B115, 333 (1976).

20. R. Brock, Phys. Rev. Lett. 44, 1027 (1980).

21. B.J. Edwards and T.D. Gottschalk, Nucl. Phys. B186, 309 (1981).

22. C.H. Lai, Phys. Rev. D18, 1422 (1978).

23. H.C. Ballagh et al., Phys. Rev. D21, 569 (1980).

24. C. Baltay et al., Phys. Rev. Lett. 39, 62 (1977).

25. H. Deden et al., Phys. Lett. 67B, 474 (1977).

26. M. Jonker et al., Preprint CERN-EP/81-95 (1981) submitted to Phys. Lett.

27. B.L.M. Peyaud et al., Proceedings of the European Physical Society, Lisbon 1981.

28. M. Holder et al., Phys. Lett. 70B 396 (1977).

29. J.G.H. deGroot et al., Phys. Lett. 86B 103 (1979).

30. K. Nishikawa et al., Phys. Rev. Lett. 46 1555 (1981). The 1μ normalization for the $\mu^-\mu^-$ data presented in these proceedings has been modified from the procedure discussed in footnote 14 of PRL 46 1555. Here there is no requirement on the hadron energy or direction for the data in Figures 13 and 16.

31. A. Benvenuti et al., Phys. Rev. Lett. 41 1204 (1978).

32. M.H. Shaevitz, Proceedings of Summer Institute on particle Physics, the Weak Interaction, edited by Anne Mosher, SLAC Report No. 239, p. 475 (1980).

33. H. Goldberg, Phys. Rev. Lett. 39 1598 (1977).

B.L. Young, T.F. Walsh, and T.C. Yang, Phys. Lett. 74B 111 (1978).

G.L. Kane, J. Smith, and J.A.M. Vermasern, Phys. Rev. D19, 1978 (1979).

34. S.J. Brodsky, C. Peterson, and N. Sakai, Phys. Rev. D23, 2745 (1981).

35. K.L. Giboni et al., Phys. Lett. 85B 437 (1979).

36. V. Barger, W.Y. Keung, and R.J.N. Phillips, Phys. Rev. D24, 244 (1981).

37. P. Avery et al., Phys. Rev. Lett. 44, 1309 (1980).

38. G.J. Feldman et al., Phys. Rev. Lett. 38, 1313 (1977).

39. Recent unpublished results from same sign dimuon production in hadronic reactions imply that D^0, $\bar{D}^0$ mixing is less than 3.2% (95% CL). To be published; A. Bodek et al., University of Rochester preprint UR-802.

40. T. Trinko et al., Phys. Rev. D23, 1889 (1981).

41. V.V. Ammosov et al., preprint IHEP 81-65, Serpukhov 1981. Submitted to Phys. Lett.

42. B. Barish, J.F. Bartlett, R. Blair, A. Bodek, R. Coleman, Y.K. Chu, D.A. Edwards, O. Fackler, Y. Fukushima, K. Jenkins, B. Jin, Q.A. Kerns, T. Kondo, J. Lee, J. Ludwig, W. Marsh, R. Messner, D. Novikoff, M. Purohit, P.A. Rapidis, F.J. Sciulli, S. Segler, M.H. Shaevitz, W.H. Smith, R. Stefanski, D. Theriot and D. Yovanovitch.